PHYSICAL REVIEW B **81**, 140407(R) (2010)

# Temperature dependence of magnetization drift velocity and current polarization in $Ni_{80}Fe_{20}$ by spin-wave Doppler measurements

M. Zhu
*Center for Nanoscale Science and Technology, National Institute of Standards and Technology, Gaithersburg, Maryland 20899, USA and Maryland Nanocenter, University of Maryland, College Park, Maryland 20742, USA*

C. L. Dennis
*Metallurgy Division, National Institute of Standards and Technology, Gaithersburg, Maryland 20899, USA*

R. D. McMichael
*Center for Nanoscale Science and Technology, National Institute of Standards and Technology, Gaithersburg, Maryland 20899, USA*

(Received 30 March 2010; published 23 April 2010)

A spin-wave Doppler technique is used to measure the temperature dependence of both the magnetization drift velocity, which represents the magnitude of adiabatic spin-transfer torque, and the current polarization in current-carrying $Ni_{80}Fe_{20}$ wires. For current densities of $10^{11}$ $A/m^2$, we obtain magnetization drift velocities decreasing from $4.8 \pm 0.3$ to $4.1 \pm 0.1$ m/s over a temperature range from 80 to 340 K. Interpretation of velocity values yields current polarization dropping from $0.75 \pm 0.05$ to $0.58 \pm 0.02$ over the same temperature range. Analysis indicates different temperature dependences for spin-up and spin-down conductivities, suggesting a strong impurity scattering of spin-down electrons.

DOI: 10.1103/PhysRevB.81.140407 PACS number(s): 75.30.Ds, 75.40.Gb, 76.50.+g, 72.25.Ba

The realization that electrical currents can carry angular momentum and that the angular momentum transfer can be used to manipulate and detect ferromagnetic order on the nanoscale has sparked great scientific and technical interest in recent years. These spin-transfer effects form a key part of the physics that supports development of new technologies such as magnetic memories[1,2] and nanoscale microwave oscillators.[3,4]

A key parameter for spin-transfer effects is the current polarization $P$ that is developed in ferromagnetic metals as spin-up and spin-down electrons carry different currents, $J_\uparrow$ and $J_\downarrow$, respectively: $P=(J_\uparrow-J_\downarrow)/(J_\uparrow+J_\downarrow)$. A critical step in the development of spin-torque switched memories will be to reduce the critical current density required to "write" a memory cell[1] and a simple model indicates that the critical current is proportional to $1/P$.[5] The current polarization is also important to technologies that involve current-driven motion of domain walls[2,6] where the domain wall velocity is proportional to $P$. As successful development of these technologies will require operation over a temperature range, not only values of $P$, but also the temperature dependence of $P$ will be important.

Despite the importance of $P$, independent measurements have produced a range of values (Table I) for the case of the ferromagnetic alloy $Ni_{80}Fe_{20}$ (Py). Some of the discrepancies between these reported values can be attributed to sample preparation, interfacial effects, and contact size effects,[7] and some are intrinsic to the different techniques yielding differently defined polarization values that correspond to different types of transport, as outlined by Mazin.[8] Spin-polarized photoemission measures the density-of-states polarization which is proportional to surface magnetization[9] while the tunneling spin polarization measured in magnetic tunnel junction depends strongly on tunneling probability.[10,11] Those measurements have already shown that different types of spin polarization have distinct temperature dependences.[9–11]

In this Rapid Communication, we report the first measurements of the temperature dependence of current polarization in $Ni_{80}Fe_{20}$. We use a current-induced spin-wave Doppler technique pioneered by Vlaminck and Bailleul[18] which has the advantages of immunity to interfacial effects at contacts, the clear identification of the result as a diffusive transport measurement in the bulk metal, and the freedom to change the temperature.

The notion that the interaction between spin waves and currents would appear in the form of a Doppler shift was suggested early,[19] and refined more recently in terms of the spin-transfer torque theory,[20,21] which is summarized here for a continuous material in terms of the Landau-Lifshitz-Gilbert equation of motion for the magnetization $\mathbf{M}$ including spin-torque terms,

$$(d/dt + \mathbf{v}\cdot\nabla)\mathbf{m} = -\mu_0|\gamma|(\mathbf{m}\times\mathbf{H}) + \alpha\mathbf{m}\times(d/dt + \mathbf{v}\cdot\nabla)\mathbf{m} + (\beta-\alpha)\mathbf{m}\times\mathbf{v}\cdot\nabla\mathbf{m}. \quad (1)$$

Here, $\mathbf{m}=\mathbf{M}/\|\mathbf{M}\|$, $\mathbf{H}$ represents applied fields and interaction

TABLE I. Summary of published values of $P$ in $Ni_{80}Fe_{20}$. Measurement temperature is 4.2 K except as noted.

| $P$ | Method | Ref. |
|---|---|---|
| $0.32 \pm 0.04$ | Spin-dependent tunneling | 12 |
| 0.48 | Spin-dependent tunneling | 13 |
| $0.37 \pm 0.05$ | Point-contact Andreev reflection | 14 |
| $0.47 \pm 0.03$ | Point-contact Andreev reflection | 15 |
| $0.76 \pm 0.07$ | Perp. current magnetoresistance | 16 |
| $0.8 \pm 0.1$ | Perp. current magnetoresistance @ 77 K | 17 |
| $0.50 \pm 0.05$ | Spin-wave Doppler @ 293 K | 18 |

 

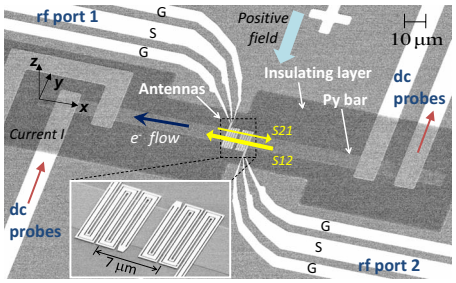


FIG. 1. (Color online) SEM image of a device with an 8 $\mu$m wide Py strip. $S_{12}$ ($S_{21}$) refers to the spin-wave transmission from rf port 2(1) to port 1(2) and electrons flow in the negative $x$ direction for positive current. In positive fields, $S_{12}$ is much stronger than $S_{21}$. The inset shows the zoomed-in image of the microwave antennas. The periodicity of the rf current is 750 nm and the center-to-center distance of the pair of antennas is 7 $\mu$m.

fields acting on the magnetization, $\gamma$ is the gyromagnetic ratio, $\alpha$ is the Gilbert damping parameter, and $\beta$ is the coefficient for the nonadiabatic spin-transfer term. The magnetization drift velocity $\mathbf{v}$ arises from adiabatic spin transfer, and is given by several authors[22,23] as,

$$\mathbf{v} = -\frac{g\mu_B P}{2M_s|e|}\mathbf{J}, \tag{2}$$

where $\mathbf{J}$ is the current density and $g \approx 2$ is the Landé $g$ factor. We obtain polarization values from values of $\mathbf{v}$, which are obtained from measured shifts in the propagation frequency of spin waves.

The theoretical basis for the measurement is a shift in the spin-wave dispersion relation $\omega(\mathbf{k})$ by an amount $\Delta\omega = \mathbf{k}\cdot\mathbf{v}$ in the presence of current. Below, we describe two methods to obtain the theoretical frequency shift from Eq. (1). First we look for a solution of Eq. (1) in the form of a spin wave, $\mathbf{m} = \mathbf{m}_0 + \delta\mathbf{m}\exp[i(\mathbf{k}\cdot\mathbf{r} - \omega t)]$, where $\delta\mathbf{m}$ is a small transverse deviation from the static, uniform ground state $\mathbf{m}_0$. Substituting this spin-wave solution into Eq. (1), the angular frequency $\omega$ always appears as $\omega - \mathbf{v}\cdot\mathbf{k}$, meaning that a spin wave with wave vector $\mathbf{k}$ that propagates at frequency $\omega(0) = \omega_\mathbf{k}$ in zero current will propagate at shifted frequency $\omega(J) = \omega_\mathbf{k} + \mathbf{v}\cdot\mathbf{k}$ in nonzero current.[18] A more complete analysis shows that the final term in Eq. (1) results in a current-dependent contribution to the spin-wave damping,[24] which we do not discuss further here.

An alternative view can be obtained by noticing that the operators $(d/dt + \mathbf{v}\cdot\nabla)$ can be replaced with $(d/dt)$ if one shifts to a reference frame that moves with velocity $\mathbf{v}$. With the exception of the final term, Eq. (1) is then equivalent to the equations of motion for zero current in this moving frame.[25] Viewed from the laboratory frame, it is clear that the spin waves will propagate as if the magnetic medium were moving with velocity $\mathbf{v}$, creating Doppler shifts expected for a moving medium.

An example of the devices we use to launch, propagate, and detect spin waves in a current-carrying Py wire is shown in Fig. 1. We first pattern 20-nm-thick Py wires with different widths using photolithography, E-beam evaporation and lift-off on high-resistivity Si wafers covered with a 20 nm $Al_2O_3$.

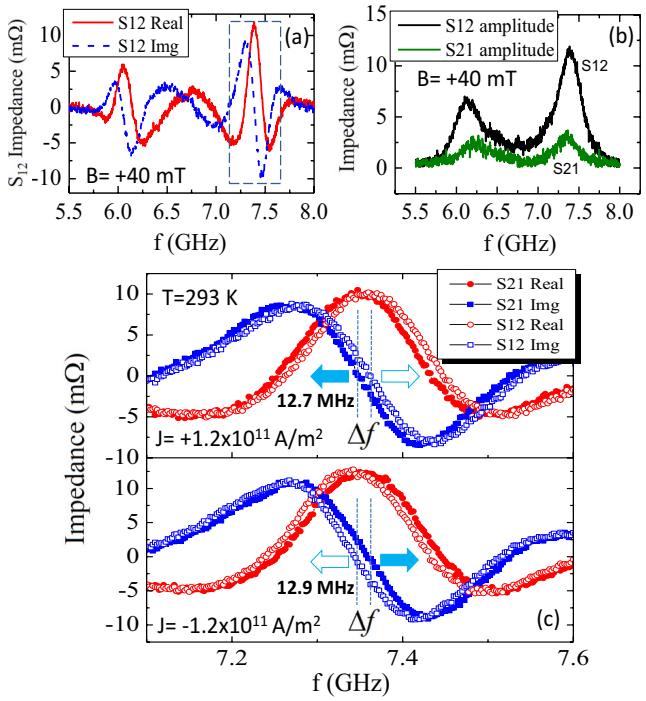


FIG. 2. (Color online) (a) Real (red solid line) and imaginary (blue dashed line) part of $S_{12}$ transmission impedance in a +40 mT field at room temperature with no dc current. (b) The amplitude of $S_{12}$ and $S_{21}$ in the same +40 mT field. (c) $S_{12}$ and $S_{21}$ transmission impedance response when a current density of $\pm 1.2\times 10^{11}$ A/m$^2$ is applied in the Py wire. The frequency shift $\Delta f$ between the $S_{12}$ and $S_{21}$ curves changes sign when the current is reversed.

We place four Cr(5 nm)/Au(100 nm) dc contacts at the ends of the Py wire as current/voltage probes, and we evaporate a 45 nm $Al_2O_3$ layer to insulate the Py wire from the antennas, which we pattern by E-beam lithography and lift-off of Cr(5 nm)/Au(150 nm).

We connect the microwave antennas to the two ports of a vector network analyzer via microwave probes which are calibrated using a short-open-load-through method with a resolution of 2.5 MHz. The antennas have periodic structures (inset of Fig. 1) that couple predominantly to spin waves of only two wave vectors:[18] $k_0 = 8.38$ $\mu$m$^{-1}$ and $k_1 = 2.79$ $\mu$m$^{-1}$ in the present case. The spin-wave transmission between the antennas has two corresponding resonances as shown in Fig. 2(a). Static fields were applied in the sample plane, perpendicular to the wire, so that the spin-wave propagation is perpendicular to the equilibrium magnetization (magnetostatic surface wave geometry).

In this configuration, there is a nonreciprocal antenna-spin-wave coupling[26] such that $S_{21}$ is relatively weak for positive fields [Fig. 2(b)], and $S_{12}$ is weak in negative fields. This effect makes detection of small frequency shifts between $S_{12}$ and $S_{21}$ difficult. To circumvent this problem, we find that we can obtain more precise measurements of frequency shift by measuring $S_{12}$ in positive field and measuring $S_{21}$ in negative field. Instrumental offsets creating differences in the magnitudes of positive and negative fields result in a small offset on the measured frequency shift and do not affect our data analysis. All measurements reported here are

made at $\pm 40$ mT which is sufficient to saturate the bulk of the stripe. The component of transmission due to spin waves is isolated by subtracting background spectra at a reference field of $\pm 100$ mT.

The high current densities required for this measurement naturally result in Joule heating of the sample. For the maximum current density of $1.6\times10^{11}$ A/m$^2$, the resistance increases by 2.8% at 293 K and by 5.7% at 100 K, corresponding to temperature increases of $\approx$20 K and $\approx$50 K, respectively. However, because $v$ is weakly temperature dependent (see below), we argue that for $T>100$ K, heating does not compromise our results significantly as long as the supplied current density is below $1.6\times10^{11}$ A/m$^2$. Larger temperature changes and increased damping that reduced signal strength precluded measurements below 80 K.

Typical spin-wave transmission impedance curves are shown in Fig. 2(a). We focus on the main resonance at $k_0=8.38$ $\mu$m$^{-1}$ (dashed box) to measure the frequency shift created by a current in the Py wire. When a dc current is passed through the Py wire, the transmitted spin-wave detected by the antenna at the fixed $k$ is frequency shifted depending on the current direction and amplitude. Figure 2(c) upper panel shows that $S_{12}$ and $S_{21}$ are shifted to higher and lower frequencies, respectively, when a positive current density of $1.2\times10^{11}$ A/m$^2$ is applied in the Py wire.[27] When the current changes direction, the shifts of $S_{12}$ and $S_{21}$ also reverse accordingly (lower panel). Frequency shift values were obtained by calculating the cross correlation of the two transmission curves yielding an uncertainty of less than 1 MHz.

Individual magnetization drift velocity values $v=\pi\Delta f/k$ at $T=220$ K are plotted as a function of current density in Fig. 3(a). The slope of the linear fit in Fig. 3(a) corresponds to a velocity of $4.4\pm0.1$ m/s for a $10^{11}$ A/m$^2$ current density. Similarly, magnetization drift velocities were extracted from the slopes of linear fits for different temperatures. The temperature dependence of velocity [Fig. 3(b)] shows a 17% increase as temperature decreases from 340 to 80 K. Since the magnetization drift velocity results from adiabatic spin-transfer torque, the temperature dependence of $v$ reported here may partially explain a decrease in critical current density for current-driven domain-wall motion that has been observed with decreasing temperature.[28]

We extract polarization values from the frequency shift observed at various temperatures and the temperature dependence of the $M\cdot t$ product measured on an unpatterned witness film [Fig. 3(c) inset]. The temperature-dependent polarization is shown in Fig. 3(c). Error bars are derived from standard deviation in linear fits of the type shown in Fig. 3(a), uncertainty in measuring Py wire width and uncertainty in superconducting quantum interference device measurement. The room-temperature polarization value of $P=0.60\pm0.02$ is in fair agreement with the results by Vlaminck *et al.*[18] From 80 K down to 340 K, the polarization increases, trending toward a value obtained by analysis of current-perpendicular transport measurements at 4.2 K.[16] Band-structure calculations of current polarization by Nadgorny *et al.*[15] in the diffusive transport case also predict a polarization value of 0.70 for $Ni_3Fe$ at low temperature.

The spin-dependent conductivities $\sigma_\uparrow$ and $\sigma_\downarrow$ can be obtained from the polarization of the current and the resistivity of the magnetic wire using

$$\sigma_\uparrow = (1+P)/2\rho \quad \text{and} \quad \sigma_\downarrow = (1-P)/2\rho. \tag{3}$$

We plot these quantities in Fig. 4(a). The spin-up conductivity, $\sigma_\uparrow$ is much larger, and decreases with increasing temperature, while the spin-down conductivity $\sigma_\downarrow$ is smaller, and temperature independent within the measurement uncertainty.

The temperature dependences of $\sigma_\uparrow$ and $\sigma_\downarrow$ can be explained in terms of spin-up, spin-down, and spin-flip resistivities $\rho_\uparrow$, $\rho_\downarrow$, and $\rho_{\uparrow\downarrow}$, respectively. In terms of these quantities,[29]

$$\sigma_\uparrow = (\rho_\downarrow + 2\rho_{\uparrow\downarrow})/[\rho_\uparrow\rho_\downarrow + \rho_{\uparrow\downarrow}(\rho_\uparrow + \rho_\downarrow)], \tag{4}$$

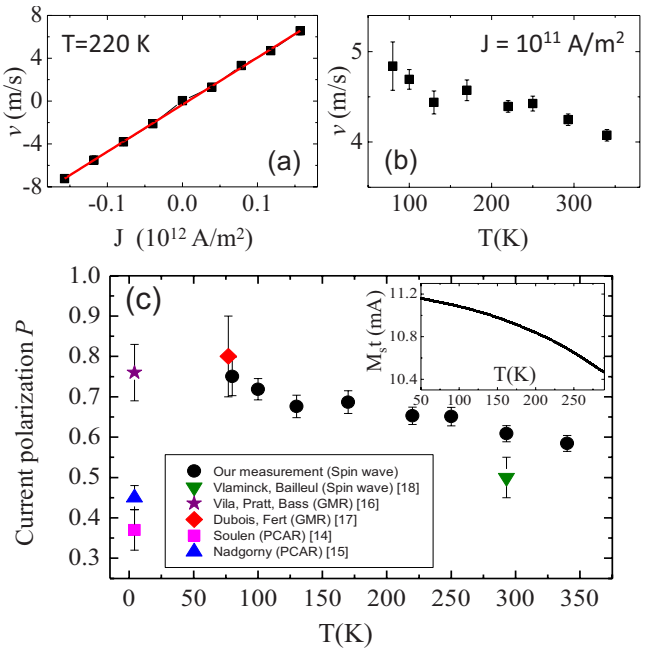


FIG. 3. (Color online) (a) Magnetization drift velocity as a function of current density ($T=220$ K). Red line is the linear fit. (b) Magnetization drift velocity from 80 to 340 K for a current density of $10^{11}$ A/m$^2$. (c) Spin polarization as a function of temperature. Some earlier measurements of spin polarization in Py are also shown for comparison. Inset shows $M_s t$ vs $T$ data.

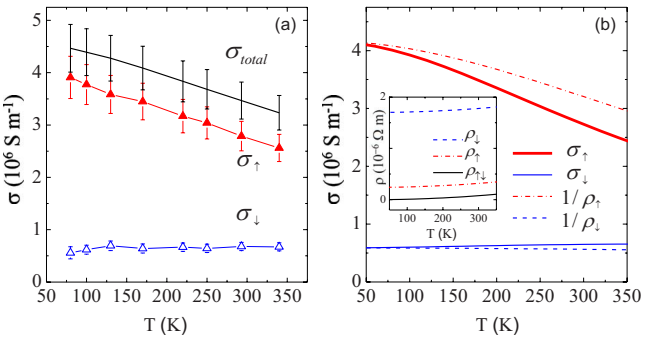


FIG. 4. (Color online) (a) Spin-up and spin-down conductivities as a function of temperature. (b) Simulated temperature dependence based on Eqs. (4) and (5) and the resistivities plotted in the inset.

$$\sigma_{\downarrow} = (\rho_{\uparrow} + 2\rho_{\uparrow\downarrow})/[\rho_{\uparrow}\rho_{\downarrow} + \rho_{\uparrow\downarrow}(\rho_{\uparrow} + \rho_{\downarrow})], \quad (5)$$

which reduce to $\sigma_i = 1/\rho_i$ if spin-flip processes are neglected.

To illustrate the behavior of these expressions, we make the assumption that the three spin-dependent resistivities all have temperature dependence of the form $\rho_i = a_i + c_i T^2$. For the low-temperature limits, resistivity measurements on dilute alloys have shown that in Ni, the low-temperature resistivity $a_i$ due to scattering from Fe atoms was 6–20 times greater for spin-down electrons than for spin-up eletrons.[30] Accordingly, we fix the ratio $a_{\downarrow}/a_{\uparrow} = 7.0$. Attributing spin-flip scattering to thermal magnons, we choose $a_{\uparrow\downarrow} = 0.0$, and although spin-flip and nonspin-flip scattering have different mechanisms, we fix $c_{\uparrow} = c_{\downarrow} = c_{\uparrow\downarrow}$. Finally, we select values of $a_{\uparrow} = 0.24\ \mu\Omega\,\mathrm{m}$ and $c_i = 8 \times 10^{-7}\ \mu\Omega\,\mathrm{m/K^2}$ that yield the low- and high-temperature limits of $\sigma_{\uparrow}$ in Fig. 4(a).

The resulting conductivity curves [Fig. 4(b)] demonstrate that spin-flip scattering reduces $\sigma_{\uparrow}$ while slightly increasing $\sigma_{\downarrow}$. Because $\rho_{\downarrow}$ is dominated by the temperature-independent term $a_{\downarrow}$, $1/\rho_{\downarrow}$ decreases only weakly with temperature. Including spin-flip scattering, however, $\sigma_{\downarrow}$ actually increases weakly with temperature in this example. On the other hand, $\sigma_{\uparrow}$ is more sensitive to phonon and magnon scattering when temperature varies.

In summary, we show that current spin polarization in $Ni_{80}Fe_{20}$ increases by 29% from 340 down to 80 K. These are the first measurements of the temperature dependence of current polarization in ferromagnetic metals. We demonstrate that the spin-wave Doppler measurement also gives a direct measure of magnetization drift velocity, which represents the amplitude of adiabatic spin-transfer torque. Analysis of spin-dependent conductivity is consistent with a strong impurity scattering for down-spin electrons.

We are grateful to Richard Kasica for help on E-beam lithography and Mark Stiles and Jacques Miltat for helpful discussions. This work was supported in part by the NIST-CNST/UMD-Nanocenter Cooperative Agreement.

[1] J. A. Katine and E. E. Fullerton, J. Magn. Magn. Mater. **320**, 1217 (2008).
[2] S. S. P. Parkin, M. Hayashi, and L. Thomas, Science **320**, 190 (2008).
[3] S. I. Kiselev, J. C. Sankey, I. N. Krivorotov, N. C. Emley, R. J. Schoelkopf, R. A. Buhrman, and D. C. Ralph, Nature (London) **425**, 380 (2003).
[4] W. H. Rippard, M. R. Pufall, S. Kaka, S. E. Russek, and T. J. Silva, Phys. Rev. Lett. **92**, 027201 (2004).
[5] J. Z. Sun, Phys. Rev. B **62**, 570 (2000).
[6] P. M. Braganca, J. A. Katine, N. C. Emley, D. Mauri, J. R. Childress, P. M. Rice, E. Delenia, D. C. Ralph, and R. A. Buhrman, IEEE Trans. Nanotechnol. **8**, 190 (2009).
[7] M. Stokmaier, G. Goll, D. Weissenberger, C. Sürgers, and H. v. Löhneysen, Phys. Rev. Lett. **101**, 147005 (2008).
[8] I. I. Mazin, Phys. Rev. Lett. **83**, 1427 (1999).
[9] D. Mauri, D. Scholl, H. C. Siegmann, and E. Kay, Phys. Rev. Lett. **62**, 1900 (1989).
[10] C. H. Shang, J. Nowak, R. Jansen, and J. S. Moodera, Phys. Rev. B **58**, R2917 (1998).
[11] B. G. Park, T. Banerjee, B. C. Min, J. G. M. Sanderink, J. C. Lodder, and R. Jansen, J. Appl. Phys. **98**, 103701 (2005).
[12] D. Paraskevopoulos, R. Meservey, and P. M. Tedrow, Phys. Rev. B **16**, 4907 (1977).
[13] R. J. M. van de Veerdonk, J. S. Moodera, and W. J. M. de Jonge, 15th ICMFS Conference Digests, 1997 (unpublished), pp. 74–75.
[14] R. J. Soulen *et al.*, Science **282**, 85 (1998).
[15] B. Nadgorny, R. J. Soulen, M. S. Osofsky, I. I. Mazin, G. Laprade, R. J. M. van de Veerdonk, A. A. Smits, S. F. Cheng, E. F. Skelton, and S. B. Qadri, Phys. Rev. B **61**, R3788 (2000).
[16] L. Vila, W. Park, J. A. Caballero, D. Bozec, R. Loloee, W. P. Pratt, and J. Bass, J. Appl. Phys. **87**, 8610 (2000).
[17] S. Dubois, L. Piraux, J. M. George, K. Ounadjela, J. L. Duvail, and A. Fert, Phys. Rev. B **60**, 477 (1999).
[18] V. Vlaminck and M. Bailleul, Science **322**, 410 (2008).
[19] P. Lederer and D. L. Mills, Phys. Rev. **148**, 542 (1966).
[20] Y. B. Bazaliy, B. A. Jones, and S.-C. Zhang, Phys. Rev. B **57**, R3213 (1998).
[21] J. Fernández-Rossier, M. Braun, A. S. Núñez, and A. H. MacDonald, Phys. Rev. B **69**, 174412 (2004).
[22] S. Zhang and Z. Li, Phys. Rev. Lett. **93**, 127204 (2004).
[23] A. Thiaville, Y. Nakatani, J. Miltat, and Y. Suzuki, Europhys. Lett. **69**, 990 (2005).
[24] S.-M. Seo, K.-J. Lee, H. Yang, and T. Ono, Phys. Rev. Lett. **102**, 147202 (2009).
[25] R. D. McMichael and M. D. Stiles, Science **322**, 386 (2008).
[26] V. E. Demidov, M. P. Kostylev, K. Rott, P. Krzysteczko, G. Reiss, and S. O. Demokritov, Appl. Phys. Lett. **95**, 112509 (2009).
[27] In calculating the current density, we used a width of 8.15 $\mu$m obtained from scanning electron microscope (SEM) imaging, and a thickness value of 12.5 nm obtained from the measured $M \cdot t$ product and an assumed magnetization value of $8 \times 10^5$ A/m.
[28] M. Laufenberg, W. Bührer, D. Bedau, P.-E. Melchy, M. Kläui, L. Vila, G. Faini, C. A. F. Vaz, J. A. C. Bland, and U. Rüdiger, Phys. Rev. Lett. **97**, 046602 (2006).
[29] A. Fert and I. A. Campbell, J. Phys. F: Met. Phys. **6**, 849 (1976).
[30] I. A. Campbell and A. Fert, *Ferromagnetic Materials* (North-Holland, Amsterdam, 1982), Vol. 3, Chap. 9.